



This is a repository copy of *Alkali activation of a high MgO GGBS – fresh and hardened properties*.

White Rose Research Online URL for this paper:
<http://eprints.whiterose.ac.uk/146693/>

Version: Accepted Version

Article:

Humad, A.M., Provis, J.L. orcid.org/0000-0003-3372-8922 and Cwirzen, A. (2018) Alkali activation of a high MgO GGBS – fresh and hardened properties. *Magazine of Concrete Research*, 70 (24). pp. 1256-1264. ISSN 0024-9831

<https://doi.org/10.1680/jmacr.17.00436>

© 2018 ICE Publishing. This is an author-produced version of a paper subsequently published in *Magazine of Concrete Research*. Uploaded in accordance with the publisher's self-archiving policy.

Reuse

Items deposited in White Rose Research Online are protected by copyright, with all rights reserved unless indicated otherwise. They may be downloaded and/or printed for private study, or other acts as permitted by national copyright laws. The publisher or other rights holders may allow further reproduction and re-use of the full text version. This is indicated by the licence information on the White Rose Research Online record for the item.

Takedown

If you consider content in White Rose Research Online to be in breach of UK law, please notify us by emailing eprints@whiterose.ac.uk including the URL of the record and the reason for the withdrawal request.



eprints@whiterose.ac.uk
<https://eprints.whiterose.ac.uk/>

Alkali-Activation of a High MgO GGBS – Fresh and Hardened Properties

Author 1

Abeer M. Humad^{1,2}, ¹Structural Engineering Division, Luleå University of Technology, Luleå, Sweden. ²Civil Engineering Department, Babylon University, Iraq. Email: abeer.humad@ltu.se

ORCID number: 0000-0002-5328-4073

Author 2

John L. Provis³, ³Department of Materials Science and Engineering, University of Sheffield, Sheffield, UK. Email: j.provis@sheffield.ac.uk, ORCID number: 0000-0003-3372-8922

Author 3

Andrzej Cwirzen¹, ¹Structural Engineering Division, Luleå University of Technology, Luleå, Sweden. Email: andrzej.cwirzen@ltu.se, ORCID number: 0000-0001-6287-2240

Abstract

In this study, concretes and pastes were produced from a high MgO ground granulated blast furnace slag (MgO content 16.1 wt.%) by alkali activation with various amounts and combinations of sodium carbonate and sodium silicate. Sodium carbonate activators tended to reduce slump compared to sodium silicate at the same dose, and, in contrast to the literature for many blast furnace slags with more moderate MgO, to shorten the initial and final setting times in comparison with concretes activated by sodium silicate for dosages less than 10 wt.%. Higher heat curing temperatures and the use of larger dosages of alkali activators resulted in higher early age cube compressive strength values. The XRD analysis of 7 and 28 days old pastes activated with sodium carbonates revealed formation of gaylussite, calcite, nahcolite and C-(A)-S-H gel. Curing at 20°C appeared to promote dissolution of gaylussite and calcite, while heat curing promoted their replacement with C-(A)-S-H, which also resulted in higher ultimate cube compressive strength values. Conversely, mixes activated with sodium silicate contained less crystalline phases and more disordered gel which strengthened the binder matrix.

Keywords: Alkali activated slag (AAS); alkali activators; workability; curing; compressive strength; setting properties.

1 1. Introduction

2 Alkali-activated concrete (AAC) has been developed and marketed as a low-CO₂ construction material,
3 but its acceptance still faces several challenges (Provis 2017). Carbon dioxide emissions reduction and
4 industrial waste valorisation could be achieved successfully by using alkali-activated slag (AAS) as an
5 alternative to Portland cement, and potentially with lower cost in regions where blast furnace slag (BFS)
6 is plentiful and activators can be readily sourced. BFS is a by-product of iron production and has some
7 latent hydraulic properties, which can develop in cementitious products when hydrated either in the
8 presence of Portland cement or in an alkaline solution (Neville 1995, Manmohan & Mehta 1981).
9 Solidified alkali-activated materials can also show desirable mechanical, engineering and durability
10 properties (Collins & Sanjayan 1999, Pacheco-Torgal et al. 2012, Provis & van Deventer 2014),
11 including high early strength if adequate preparation and curing conditions are adopted.

12 The chemical composition of BFS and its fineness strongly influence the fresh and hardened properties
13 of alkali activated materials (Douglas & Brandstetr 1990, Winnefeld et al. 2015, Bernal et al. 2011).
14 Similarly, the type and the amount of alkali activator, the water/precursor ratio, mixing and curing
15 procedures control both fresh and hardened matrix properties (Provis & van Deventer 2014). The
16 relatively high content of calcium in BFS compared to most other precursor used in alkali activation
17 promotes formation of Al-substituted C-S-H (C-(A)-S-H) gel (Bernal & Provis 2014, Wang & Scrivener
18 1995), though rapid dissolution and release of Ca, Si and Al. Activation of MgO-rich BFS by alkali silicate
19 (Bernal 2016) tends to produce C-A-S-H type gel as the main binding phase and Mg-Al layered double
20 hydroxide as the secondary phase; if an alkali carbonate alkali activator is used, calcium-rich carbonate
21 phases are also observed. In general, the tendency of BFS to dissolve and the consequent reaction
22 intensity increase with alkali concentration up to a certain point but not beyond this, (Nath & Sarker
23 2014) and excessive alkali dose can cause a reduction in 28-day compressive strength of alkali
24 activated concretes. Sodium hydroxide (NaOH), sodium silicate ($\text{Na}_2\text{O} \cdot r\text{SiO}_2$), sodium carbonate
25 (Na_2CO_3) and sodium sulphate (Na_2SO_4) are the activators most commonly used for alkali activation of
26 BFS. The use of sodium silicate to activate blast furnace slags of normal composition (Fernández-
27 Jiménez et al. 2003) tends to yield a denser microstructure and results in better mechanical properties,
28 particularly at early age, in comparison with mixes activated with NaOH or Na_2CO_3 . Alkali activation of
29 BFS leads to incorporation of Al ions by the C-S-H gel, which forms the main binder phase in these

30 cements, and results in longer chains of C-A-S-H with two dimensional structures and periodic inter-
31 chain cross-links. Aluminium uptake depends on the concentration of alkalis, and has been reported to
32 be more extensive at higher temperature and humidity (Schilling et al. 1994). XRD analysis of BFS
33 activated with sodium hydroxide and sodium silicate (Brough & Atkinson 2002) shows formation of low
34 quantities of crystalline phases. The silica to alkali ratio of the activator ($\text{SiO}_2/\text{Na}_2\text{O}$ ratio, denoted M_s ,
35 and with numerically very similar values whether defined as molar or mass ratio) is one of the key
36 parameters defining the properties of alkali activated BFS. M_s values between 0.75-1.5 often produce
37 the best mechanical properties across a range of curing conditions slag compositions, although the
38 details of the mix formulation do play a significant role in defining the optimal activator modulus.

39 Sodium carbonate as an activator can raise the pH value of the pore solution of AAS concrete (Bernal
40 et al. 2015) to similar values as observed in Portland cement concrete. It can also be considered more
41 environmentally friendly, is cheaper and more widely available (Provis & van Deventer 2014, Bernal
42 2016), either as a secondary product from industrial processes or by mining alkali carbonate deposits
43 followed by moderate temperature thermal treatment. The sodium carbonate is considered a weaker
44 activator mainly because the reaction of Ca^{2+} from slag with CO_3^{2-} from the activator, which favours
45 formation of calcite, must take place before the pH increases to the level (Bernal et al. 2015), which will
46 induce silica dissolution and the formation of C-A-S-H. Blending of sodium silicate with sodium
47 carbonate as activators increased the pore solution pH and induced faster reaction of slag, compared
48 to when using sodium carbonate. However, these results have largely been obtained for slags with MgO
49 contents < 10% (Ke et al. 2016), and it is known that high-magnesia slags can behave very differently
50 from those in the low-MgO compositional rang during alkali activation, so it is important to investigate
51 their response in the presence of different activators.

52 Research on fresh concrete properties for AAS activated is rather limited compared to the
53 understanding of the material in the hardened state, but in general the available test results show that
54 workability and the setting time are strongly affected by alkali content, modulus and the amount of slag
55 (Qureshi & Ghosh 2013, Lee & Lee 2013).

56 The setting process of AAS concretes tends to show progressive and gradual stiffening, evidenced in
57 engineering tests as a rather fast slump loss but not always rapidly reaching a fully set condition. An
58 increased activator dosage (Živica 2007) tends to shorten the setting time.

59 The main objective of this study is to evaluate the effect of alkali activator type on the workability and
60 setting time of alkali activated concretes based on a high-MgO blast furnace slag. Most previous studies
61 were performed using low-MgO slag which appeared to produce mixes with significantly different
62 properties from those produced from the high-Mg slag used here. The secondary objective is to
63 determine the effects of curing temperature on the mechanical properties of these mixes, especially at
64 early age. This will provide valuable information to underpin the full-scale deployment of alkali-activated
65 concretes based on a wider range of slag chemistries than in currently the case in practice.

66 **Materials and Methods**

67 Ground granulated blast furnace slag (GGBFS, Merit 5000) provided by MEROX, Sweden was used in
68 this study. The chemical composition of the slag shown in Table 1 was determined using a Panalytical
69 Zetium XRF spectrometer. The physical properties were provided by the supplier. The mix proportions
70 of the concretes studied are shown in Table 2. All concretes contained 450 kg/m³ of GGBFS, and all
71 the samples had water/slag w/s mass ratios of 0.45 for concretes, and 0.36 for pastes. The alkali
72 activators used were: powdered anhydrous sodium carbonate (abbreviated SC) provided by CEICH SA
73 (Poland), and liquid sodium silicate (SS) provided by PQ Corporation. The SS had alkali modulus Ms
74 (by mass) SiO₂/Na₂O=2.2, with 34.37 wt.% SiO₂, 15.6 wt.% Na₂O and a solids content of 49.97 wt.%.
75 Some mixes were activated with sodium silicate solutions of modulus 1 and 1.5, adjusted from the
76 commercial SS by addition of sodium hydroxide pellets. The sodium hydroxide pellets had 98.5% purity
77 and were also provided by PQ Corporation. The alkali activator doses used were 3, 5, 10 and 14 wt.%
78 by mass of binder. In addition, a mixture of 5 wt.% sodium silicate and 5 wt.% sodium carbonate (by
79 binder mass) was used, Table 2. The total aggregate content was 1663 kg/m³ in all concretes. The all-
80 in aggregates used were natural granite from Piteå, Sweden, and had particle size 0-8 mm, with a fine
81 content of 70 wt.%.

82 The mixing procedure commenced with mixing of all dry ingredients for 3 minutes. Powdered sodium
83 carbonate and/or liquid sodium silicate were combined with any additional mix water and left to stand

84 for one hour (to dissolve or equilibrate, respectively) before being added to the mixed dry materials, and
85 then mixed for another 4 minutes. The slump was determined following ASTM C143 (ASTM
86 International 2015). Cube specimens for compressive strength testing were casted into alkali-resistant
87 polymer 100 mm cube moulds. Immediately after casting, the samples were sealed with plastic bags.
88 Curing was carried out by two procedures. In the first procedure specimens were sealed and kept at
89 $20\pm 2^{\circ}\text{C}$ and 40-45% relative humidity (RH) until testing, while in the second procedure sealed
90 specimens were heat cured at 65°C for 24 hours then stored and kept sealed at $20\pm 2^{\circ}\text{C}$ and 40% RH
91 until testing. No weight changes were recorded. Sealing of specimens was done by tight wrapping in a
92 plastic foil.

93 Initial and final setting times were determined following the IS 4031 implementation of the Vicat test (IS:
94 4031-PART 5-1988), measuring penetration using a 1-mm diameter needle and a plunger mass of 300
95 g. Initial set is defined to be reached when the penetration is 5-7mm from the bottom, and final set when
96 there is no longer any visible penetration of the outer circle. Cube compressive strength was determined
97 at 1, 7 and 28_days after casting, following SS-EN 12390-3 (SS-EN 12390-3). The loading rate was set
98 to 10 kN/sec. The pH values of activator solutions were measured using a digital pH meter (HANNA-
99 HI208). The XRD analysis was conducted on 7 and 28-day old powdered paste samples using a
100 PANalytical Empyrean XRD unit operating with Cu $K\alpha$ radiation, with step size $0.0262^{\circ} 2\theta$ and total
101 scanning time for each sample 16 minutes, with results evaluated using the HighScore Plus software.

102

103 **2. Results and discussion**

104 **3.1 Fresh state properties**

105 The type and amount of alkali activators strongly affected the fresh concrete properties. Mixes activated
106 with SS generally had higher slump in comparison with SC-activated mixes, most probably due to the
107 lubricating and dispersant effect of dissolved silicate, as also observed in the literature (Fernández-
108 Jiménez et al. 2003, Rajesh et al. 2013), Figures 1-A and 2. Similar behaviour occurred in the mix
109 activated with 5wt.% SS + 5wt.% SC. Higher dosages tended to strengthen this effect but also resulted
110 in later rapid loss of workability (Figures 1 and 2), also consistent with previous studies (Fernández-

111 Jiménez et al. 2003, Rajesh et al. 2013). All mixes showed a progressive loss of workability (slump
112 loss) which was more pronounced when 14wt.% of SS or SC were used, Figure 1-B.

113 A decrease in the SS alkali modulus from 2.2 to 1 resulted in an increase in both slump and measured
114 pH values, which can be related to the effective increase of the Na₂O content which initiates the
115 dissolution of slag grains, Figure 3, and also the lower viscosity of a lower-modulus silicate solution
116 (Vail 1952). A higher pH value of the alkaline solution is known to enhance the dissolution rate of slag
117 and thus to accelerate this step of the hydration process (Kovtun et al. 2015), this effect is sufficient to
118 overcome the reduction in the content of dissolved silicate (which has a plasticising action as mentioned
119 above), and so gives an increased slump, Figure 1-A. Fresh concrete properties, and especially the
120 loss of workability, are directly linked to the recorded initial and final setting times, Figure 4-A and B.

121 Generally, mixes activated with 3 and 5 wt.% SS, showed the longest initial setting times, exceeding
122 230 minutes, independent of Ms, although these concretes also showed very low slump (Figure 1-A).
123 Concretes activated with SC and concretes activated with higher amounts of SS (10 and 15 wt.%) had
124 short initial setting times of between 25 and 50 minutes. The increase of the modulus Ms appeared to
125 shorten the initial setting time, Figure 4A, which can be related to more intense dissolution of silica and
126 alumina (Chang 2003). However, a decrease of the modulus of the SS from 2.2 to 1.0, at a dose of 3
127 wt.% caused the shortening of the final setting time from 120 to 78 hours, but these values were the
128 longest final setting times among all the mixes tested. A decrease in the amount of SC resulted in a
129 longer final setting time, and the combination of SC and SS in mix SC5-SS5 gave the initial setting after
130 100 minutes and the final setting after 50 hours.

131 Generally, mixes with higher alkali contents, showed shorter initial and final setting times, whether
132 activated with SC or SS. This could be directly related to the higher alkalinity of these systems which
133 caused faster and more extensive dissolution of the slag followed by a more intense precipitation of
134 reaction products at early stages (Chang 2003, Bernal et al. 2011). The observed rapid loss of
135 workability in the case of mix SC14 can be related to the initiation of C-A-S-H formation. Earlier studies
136 indicate that even the usage of a retarder did not prevent loss workability of similar mixes after 30 min
137 (Collins & Sanjayan 1998), a similar timeframe to the results shown here in Figure 1-B. Formation of
138 hydrotalcite within the reaction products is controlled significantly by the MgO content of the slag; due
139 to the high concentration of MgO (16.1 wt.%) in the ground granulated blast furnace slag used in this

140 work, much more extensive formation of this phase at early age may have contributed to the short initial
141 setting time and accelerated the kinetics of reaction, particularly when SC was the activator (Ke et al.
142 2016).

143

144 **3.2 Hardened state properties**

145 The compressive strength results are shown in Figures 5-7. In general, a higher dose of alkali activators
146 led to increased 1, 7 and 28-day cube strength values. The 1-day cube strength was higher for heat
147 cured specimens, Figure 5, due to the increased dissolution of BFS and acceleration of the formation
148 of strength-giving reaction products (Bakharev et al. 1999a). The lab cured specimens ($20\pm 2^\circ\text{C}$)
149 activated with 14 wt.% SS having $M_s=1$, and those with <14 wt.% SC, were not yet hard after one day
150 of curing. After 7 days of lab curing cube strength values varied between 10 to 48 MPa, and between
151 16 and 60 MPa after 28 days. Longer curing times are known to promote further strength progress in
152 ambient- cured specimens activated with both silicate and carbonate solution, as the slag continuous
153 to progressively react with highly alkaline pore solution (Bernal et al. 2016).

154 The 28 day old concretes cured at 20°C and activated with SC, or with 3 and 5 wt.% SS, showed higher
155 final (28 day) cube strength values than heat cured mixes. Similar trends are common for OPC
156 concretes (Verbeck & Helmuth 1968), as the lower curing temperature allows the development of a
157 more mature final microstructure. Conversely, mixes activated with 10 and 14 wt.% of SS showed higher
158 strength values when heat cured. Similar observations in the past for alkali-activated slags have been
159 related to the decreased crystallinity of the C-A-S-H (Wang & Scrivener 2003), and also an inferred
160 higher amount of aluminosilicate gel formation (Wang et al. 1994). The literature also indicates that heat
161 curing tends to coarsen the pore structure due to a higher reaction rate for C-A-S-H, in comparison with
162 the rate of diffusion, resulting in formation of interstitial pores in between denser precipitates to form a
163 barrier that prevents further dissolution and dispersion of ions (Bakharev et al. 1999b). The present test
164 results indicate that this possible coarsening of the microstructure could be overcome, at least at high
165 activator doses, by the formation of stronger reaction products (and potentially related also to higher
166 solubility in the more alkaline pore solution) which yield higher ultimate cube strength values.

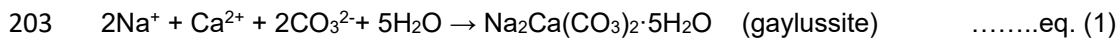
167 The type and the relative amounts of phases formed by alkali-activation of BFS depend largely on the
168 composition of the alkali activator and the BFS (Myers et al. 2017). The high MgO content of over 16

169 wt.%, present in the BFS used in this study BFS accelerates the kinetics of reaction and promotes
170 formation of hydrotalcite group minerals (Bernal 2016) as detected by XRD here, Figures 8 and 9. Other
171 reaction product phases detected by XRD include tobermorite-like C-A-S-H gels, as well as the
172 carbonate phases gaylussite ($\text{Na}_2\text{Ca}(\text{CO}_3)_2 \cdot 5\text{H}_2\text{O}$), nahcolite (NaHCO_3) and calcite (CaCO_3). The HT
173 was observable as a crystalline reaction product only in heat cured mixes activated with SS, and in
174 mixes activated with 14 wt.% SC (both heat and lab cured), but may have been present in a disordered
175 form in other samples. The XRD results show the presence of C-(A)-S-H gels in all mixes at all ages
176 studied, where aluminium is incorporated into the silicate chains of the C-S-H structure (Wang &
177 Scrivener 2003, Richardson et al. 1994). This incorporation, even at early ages, results in longer chain
178 length in sodium silicate-activated slags than in hydrated C_3S or Portland cement systems (Wang &
179 Scrivener 2003, Myers et al. 2013). Mixes activated with high dosages of sodium carbonate showed
180 the predominant formation of nahcolite, calcite and gaylussite which seem to be favoured over
181 development of ordered structures within the C-(A)-S-H gel. This can be related to the reaction of Ca^{2+}
182 from slag with CO_3^{2-} from SC leading to its consumption from the solution, resulting in a lower degree
183 of formation as it is thus not available to react initially with dissolved silica (Bernal et al. 2015).

184 The type of gel formed is affected by the pH of the activating solution and the calcium content in the
185 system. Systems with pH over 12 and a high calcium content binder (i.e. those based on BFS, as is the
186 case here) tend to show formation of C-A-S-H in preference to N-A-S-H gel (Garcia-Lodeiro et al. 2011,
187 Palomo et al. 2014). Here, the mixes activated with sodium silicate had higher pH values than those
188 activated with sodium carbonate, Table 2. As shown in Table 1 the slag used here had a relatively high
189 content of MgO (16.1 wt.%). The MgO drives the removal of carbonate species from the activator, and
190 then from the pore solution if any remains after setting, through formation of hydrotalcite-group phases
191 and therefore makes the calcium available for formation of the dominant C-(A)-S-H gel (Ke et al. 2016).

192 The observed gaylussite tends to form at a very early age, even prior to initiation of C-A-S-H formation
193 (Fernández-Jiménez & Puertas 2001), due to the easier breakage of O-Ca bonds at lower pH in
194 comparison with O-Al and O-Si bonds (Ke et al. 2016, Bernal et al. 2015). As shown in Eq. (1), a high
195 dosage of sodium carbonate will provide an excess of Na ions, which will support gaylussite formation.
196 From Figures 8 and 9, gaylussite showed a weaker presence in the XRD data with increasing time of
197 curing (7 and 28 days), as it is considered a transient phase in sodium-carbonate activated slag binders,

198 forming initially but then being consumed, and its consumption is related to the development of more
199 stable carbonates (Ke et al. 2016). Usually, once the C-A-S-H starts to form the gaylussite will tend to
200 dissolve. However, the results presented here indicate that the combination of a higher dosage of
201 sodium carbonate and laboratory curing at 20°C could slow down or limit the dissolution process of
202 gaylussite, some of which could still remain in the hardened binder matrix even after 28 days of curing.



204 Gaylussite was detected in 7 and 28-day old mixes activated with 14 wt.% SC, and with the combination
205 of 5wt.% SS and 5wt.% SC under both lab and heat curing. In the previous study of Bernal (Bernal et
206 al. 2016) using a mixed carbonate-silicate activator, pirssonite (a less-hydrous sodium-calcium mixed
207 carbonate) was formed instead of gaylussite, but the observation of a carbonate double salt here is
208 nonetheless consistent with that previous work.

209

210 **4. Conclusions**

211 The effects of carbonate activators and curing temperatures on alkali activated slag concretes produced
212 from a high-MgO slag were studied. Key findings include:

- 213 • Concrete mixes activated with sodium silicate had a generally higher slump than with mixes activated
214 with sodium carbonate due to the plasticity effect of the sodium silicate.
- 215 • Workability loss was more rapid for sodium carbonate activated mixes produced using this slag; this
216 differs from results for lower-Mg slags where sodium carbonate-activated mixes often remain fluid for a
217 much longer period, and then set only slowly. The workability of the AAS concrete mix activated by 14%
218 SC has been lost after 12 minutes of mixing with water. It would be impossible to use that concrete mix
219 for in-situ concrete produced in the factory and transported over a long distance. However, 12 minutes
220 may be a sufficiently long working time for some precast concrete production of small size products,
221 e.g. tiles or bricks, in a rapid process.

- 222 • AAS pastes activated by sodium carbonate have shorter initial and final setting time than pastes
223 activated by sodium silicate; the setting times decrease with increasing activator dosage, and with
224 decreasing $\text{SiO}_2/\text{Na}_2\text{O}$ ratio in sodium silicate.
- 225 • The combination of 5 wt.% sodium silicate + 5 wt.% sodium carbonate as activator appeared to
226 increase the slump, initial and final setting time with no substantial loss of early or later compressive
227 strength.
- 228 • Heat curing and higher dosages of alkali activators produced higher early age and ultimate cube
229 strength values, and appeared to mitigate the loss of final strength that was induced by heat curing of
230 concrete with lower activator dose.
- 231 • 28-day old pastes contain C-(A)-S-H, hydrotalcite-group phases and carbonates including gaylussite,
232 nahcolite and calcite as reaction products.
- 233 • Curing at 20°C promotes dissolution of gaylussite and calcite; heat curing promotes the replacement
234 of gaylussite with C-(A)-S-H, which resulted in higher ultimate cube strength values.
- 235 • Mixes activated with sodium silicate contain less crystalline phases and more disordered C-A-H gel,
236 which strengthened the binder matrix. Some traces of ordered C-A-S-H phases were observed, but only
237 at lower dosages of sodium silicate or when sodium carbonate was used as a co-activator.

238 **Acknowledgements**

239 This research was funded by the Iraqi Ministry of Higher Education and Scientific Research, Iraq. The
240 authors would like to thank the technical staff of the laboratory at LTU, Sweden, and Dr Oday Hussein
241 and Dr Xinyuan Ke (University of Sheffield) for conducting the XRF analysis.

242 **References**

243

244 ASTM (2015) C143/C143M-15a: Standard test method for slump of hydraulic-cement concrete. ASTM
245 International, West Conshohocken, PA, USA.

246 Bakharev, T., Sanjayan, J. & Cheng, Y. 1999a, "Effect of elevated temperature curing on properties of
247 alkali-activated slag concrete", *Cement and Concrete Research*, vol. 29, no. 10, pp. 1619-1625.

- 248 Bakharev, T., Sanjayan, J.G. & Cheng, Y. 1999b, "Alkali activation of Australian slag cements",
249 *Cement and Concrete Research*, vol. 29, no. 1, pp. 113-120.
- 250 Bernal, S.A., de Gutiérrez, R.M., Pedraza, A.L., Provis, J.L., Rodriguez, E.D. & Delvasto, S. 2011,
251 "Effect of binder content on the performance of alkali-activated slag concretes", *Cement and*
252 *Concrete Research*, vol. 41, no. 1, pp. 1-8.
- 253 Bernal, S.A. & Provis, J.L. 2014, "Durability of alkali-activated materials: progress and perspectives",
254 *Journal of the American Ceramic Society*, vol. 97, no. 4, pp. 997-1008.
- 255 Bernal, S.A., Provis, J.L., Myers, R.J., San Nicolas, R. & van Deventer, J.S. 2015, "Role of
256 carbonates in the chemical evolution of sodium carbonate-activated slag binders", *Materials and*
257 *Structures*, vol. 48, no. 3, pp. 517-529.
- 258 Bernal, S.A., San Nicolas, R., van Deventer, J.S. & Provis, J.L. 2016, "Alkali-activated slag cements
259 produced with a blended sodium carbonate/sodium silicate activator", *Advances in Cement*
260 *Research*, vol. 28, no. 4, pp. 262-273.
- 261 Bernal, S.A. 2016, "Advances in near-neutral salts activation of blast furnace slags", *RILEM Technical*
262 *Letters*, vol. 1, pp. 39-44.
- 263 Brough, A. & Atkinson, A. 2002, "Sodium silicate-based, alkali-activated slag mortars: Part I. Strength,
264 hydration and microstructure", *Cement and Concrete Research*, vol. 32, no. 6, pp. 865-879.
- 265 Chang, J. 2003, "A study on the setting characteristics of sodium silicate-activated slag pastes",
266 *Cement and Concrete Research*, vol. 33, no. 7, pp. 1005-1011.
- 267 Collins, F. & Sanjayan, J. 1999, "Workability and mechanical properties of alkali activated slag
268 concrete", *Cement and Concrete Research*, vol. 29, no. 3, pp. 455-458.
- 269 Collins, F. & Sanjayan, J. 1998, "Early age strength and workability of slag pastes activated by NaOH
270 and Na₂CO₃", *Cement and Concrete Research*, vol. 28, no. 5, pp. 655-664.
- 271 Douglas, E. & Brandstetr, J. 1990, "A preliminary study on the alkali activation of ground granulated
272 blast-furnace slag", *Cement and Concrete Research*, vol. 20, no. 5, pp. 746-756.
- 273 Fernández-Jiménez, A., Puertas, F., Sobrados, I. & Sanz, J. 2003, "Structure of calcium silicate
274 hydrates formed in alkaline-activated slag: influence of the type of alkaline activator", *Journal of*
275 *the American Ceramic Society*, vol. 86, no. 8, pp. 1389-1394.
- 276 Fernández-Jiménez, A. & Puertas, F. 2001, "Setting of alkali-activated slag cement. Influence of
277 activator nature", *Advances in Cement Research*, vol. 13, no. 3, pp. 115-121.
- 278 Garcia-Lodeiro, I., Palomo, A., Fernández-Jiménez, A. & Macphee, D. 2011, "Compatibility studies
279 between NASH and CASH gels. Study in the ternary diagram Na₂O–CaO–Al₂O₃–SiO₂–H₂O",
280 *Cement and Concrete Research*, vol. 41, no. 9, pp. 923-931.
- 281 Ke, X., Bernal, S.A. & Provis, J.L. 2016, "Controlling the reaction kinetics of sodium carbonate-
282 activated slag cements using calcined layered double hydroxides", *Cement and Concrete*
283 *Research*, vol. 81, pp. 24-37.
- 284 Kovtun, M., Kearsley, E.P. & Shekhovtsova, J. 2015, "Chemical acceleration of a neutral granulated
285 blast-furnace slag activated by sodium carbonate", *Cement and Concrete Research*, vol. 72, pp.
286 1-9.

- 287 Lee, N. & Lee, H. 2013, "Setting and mechanical properties of alkali-activated fly ash/slag concrete
288 manufactured at room temperature", *Construction and Building Materials*, vol. 47, pp. 1201-1209.
- 289 Manmohan, D. & Mehta, P. 1981, "Influence of pozzolanic, slag, and chemical admixtures on pore
290 size distribution and permeability of hardened cement pastes", *Cement, Concrete and
291 Aggregates*, vol. 3, no. 1, pp. 63-67.
- 292 Myers, R.J., Bernal, S.A. & Provis, J.L. 2017, "Phase diagrams for alkali-activated slag binders",
293 *Cement and Concrete Research*, vol. 95, pp. 30-38.
- 294 Myers, R.J., Bernal, S.A., San Nicolas, R. & Provis, J.L. 2013, "Generalized structural description of
295 calcium–sodium aluminosilicate hydrate gels: the cross-linked substituted tobermorite model",
296 *Langmuir*, vol. 29, no. 17, pp. 5294-5306.
- 297 Nath, P. & Sarker, P.K. 2014, "Effect of GGBFS on setting, workability and early strength properties of
298 fly ash geopolymer concrete cured in ambient condition", *Construction and Building Materials*,
299 vol. 66, pp. 163-171.
- 300 Neville, A.M. 1995, *Properties of concrete, 5th Ed.*, Pearson Education, Harlow, UK.
- 301 Pacheco-Torgal, F., Abdollahnejad, Z., Camões, A., Jamshidi, M. & Ding, Y. 2012, "Durability of
302 alkali-activated binders: a clear advantage over Portland cement or an unproven issue?",
303 *Construction and Building Materials*, vol. 30, pp. 400-405.
- 304 Palomo, A., Krivenko, P., Garcia-Lodeiro, I., Kavalerova, E., Maltseva, O. & Fernández-Jiménez, A.
305 2014, "A review on alkaline activation: new analytical perspectives", *Materiales de Construcción*,
306 vol. 64, no. 315, #e022.
- 307 Provis, J.L. & van Deventer, J.S.J. (eds.) 2014, *Alkali Activated Materials, State of the Art Report*,
308 *RILEM TC 224-AAM*, Springer/RILEM, Dordrecht.
- 309 Provis, J.L. 2017, "Alkali-activated materials". *Cement and Concrete Research*, in press, DOI
310 [10.1016/j.cemconres.2017.02.009](https://doi.org/10.1016/j.cemconres.2017.02.009)
- 311 Qureshi, M.N. & Ghosh, S. 2013, "Workability and setting time of alkali activated blast furnace slag
312 paste", *Advances in Civil Engineering Materials*, vol. 2, no. 1, pp. 62-77.
- 313 Rajesh, D., Narender Reddy, A., Venkata Tilak, U. & Raghavendra, M. 2013, "Performance of alkali
314 activated slag with various alkali activators", *International Journal of Innovative Research in
315 Science, Engineering and Technology*, vol. 2, no. 2, pp. 378-386.
- 316 Richardson, I., Brough, A., Groves, G. & Dobson, C. 1994, "The characterization of hardened alkali-
317 activated blast-furnace slag pastes and the nature of the calcium silicate hydrate (CSH) phase",
318 *Cement and Concrete Research*, vol. 24, no. 5, pp. 813-829.
- 319 Schilling, P.J., Butler, L.G., Roy, A. & Eaton, H.C. 1994, "²⁹Si and ²⁷Al MAS-NMR of NaOH-activated
320 blast-furnace slag", *Journal of the American Ceramic Society*, vol. 77, no. 9, pp. 2363-2368.
- 321 Vail, J.G. 1952, *Soluble Silicates: Their Properties and Uses*. American Chemical Society Monograph
322 Series, Reinhold, New York.
- 323 Verbeck, G.J. & Helmuth, R.H. 1968, "Structures and physical properties of cement paste",
324 *Proceedings of the Fifth International Symposium on the Chemistry of Cement*, Tokyo, Japan,
325 vol. 3, pp. 1-44.

- 326 Wang, S. & Scrivener, K.L. 2003, "²⁹Si and ²⁷Al NMR study of alkali-activated slag", *Cement and*
327 *Concrete Research*, vol. 33, no. 5, pp. 769-774.
- 328 Wang, S., Scrivener, K.L. & Pratt, P. 1994, "Factors affecting the strength of alkali-activated slag",
329 *Cement and Concrete Research*, vol. 24, no. 6, pp. 1033-1043.
- 330 Wang, S. & Scrivener, K.L. 1995, "Hydration products of alkali activated slag cement." *Cement and*
331 *Concrete Research*, vol. 25, no. 3, pp. 561-571.
- 332 Winnefeld, F., Ben Haha, M., Le Saout, G., Costoya, M., Ko, S. & Lothenbach, B. 2015, "Influence of
333 slag composition on the hydration of alkali-activated slags", *Journal of Sustainable Cement-*
334 *Based Materials*, vol. 4, no. 2, pp. 85-100.
- 335 Živica, V. 2007, "Effects of type and dosage of alkaline activator and temperature on the properties of
336 alkali-activated slag mixtures", *Construction and Building Materials*, vol. 21, no. 7, pp. 1463-
337 1469.
- 338
- 339
- 340
- 341

342 List of Figure and Table Captions

343

344 Table 1: Details of GGBFS used in this work.

345 Table 2: Mix proportions tests.

346 Figure 1: effect of activator type and its proportion on workability, A: Slump test results after mixing
347 about 6 min, B: workability loss of mixes with 14% sodium silicate SS and 14% sodium carbonate SC.

348 Figure 2: Results of slump testing of mixes with sodium silicate activator.

349 Figure 3: Relationship between M_s and the measured pH of the sodium silicate activator solution.

350 Figure 4: A: initial setting times for AAS pastes in minutes; B: final setting times for AAS pastes in
351 hours.

352 Figure 5: 1 day compressive cube strength results for concretes.

353 Figure 6: 7 day compressive cube strength results for concretes.

354 Figure 7: 28 day compressive cube strength results for concretes.

355 Figure 8: XRD results for 28 day old AAS pastes activated with SC. Suffix L28 denotes 28 days of lab
356 curing and H28 denotes 28 days of heat curing.

357 Figure 9: XRD results for 28 day old AAS pastes activated with SS. Suffix L28 denotes 28 days of lab
358 curing and H28 denotes 28 days of heat curing.

359

360

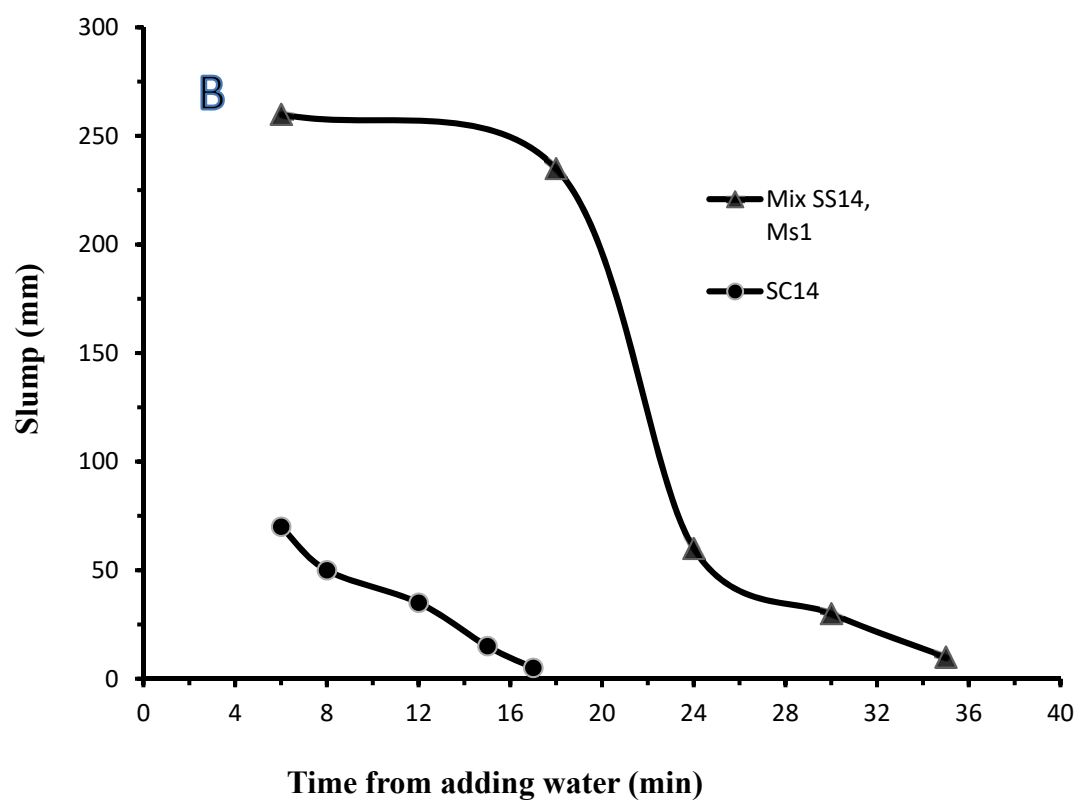
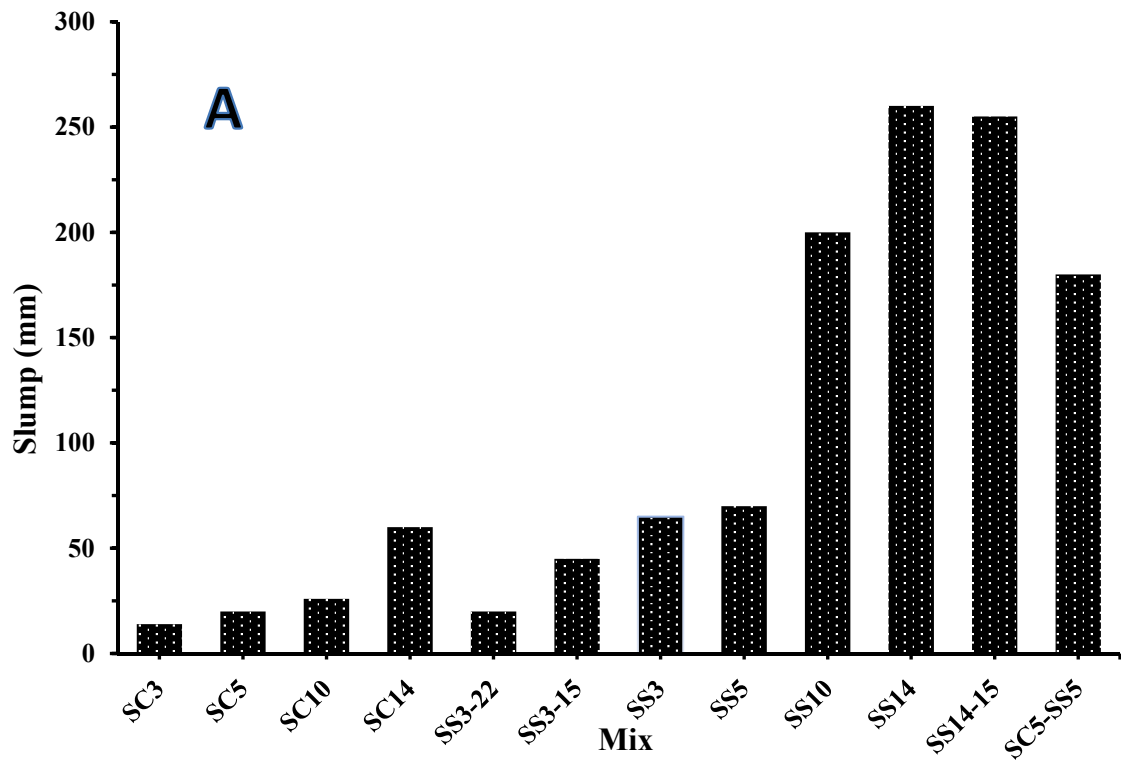
361

362

363

364

365



W

Figure 1: Effect of activator type and its proportion on workability, A: Slump test results after mixing about 6 min, B: workability loss of mixes with 14% sodium silicate SS and 14% sodium carbonate SC.

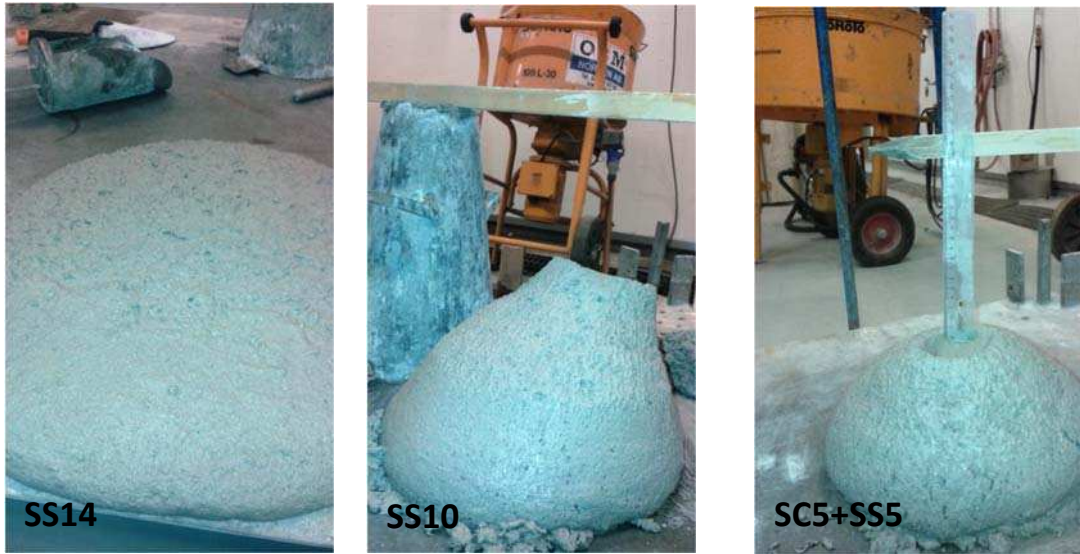


Figure 2: Results of slump testing of mixes with sodium silicate activator.

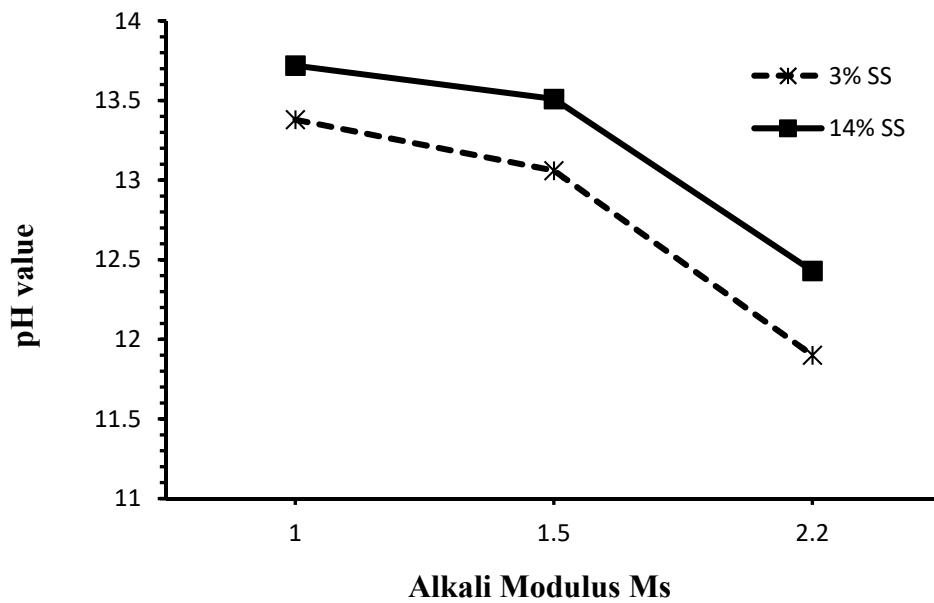


Figure 3: Relationship between M_s and the measured pH of the sodium silicate activator solution.

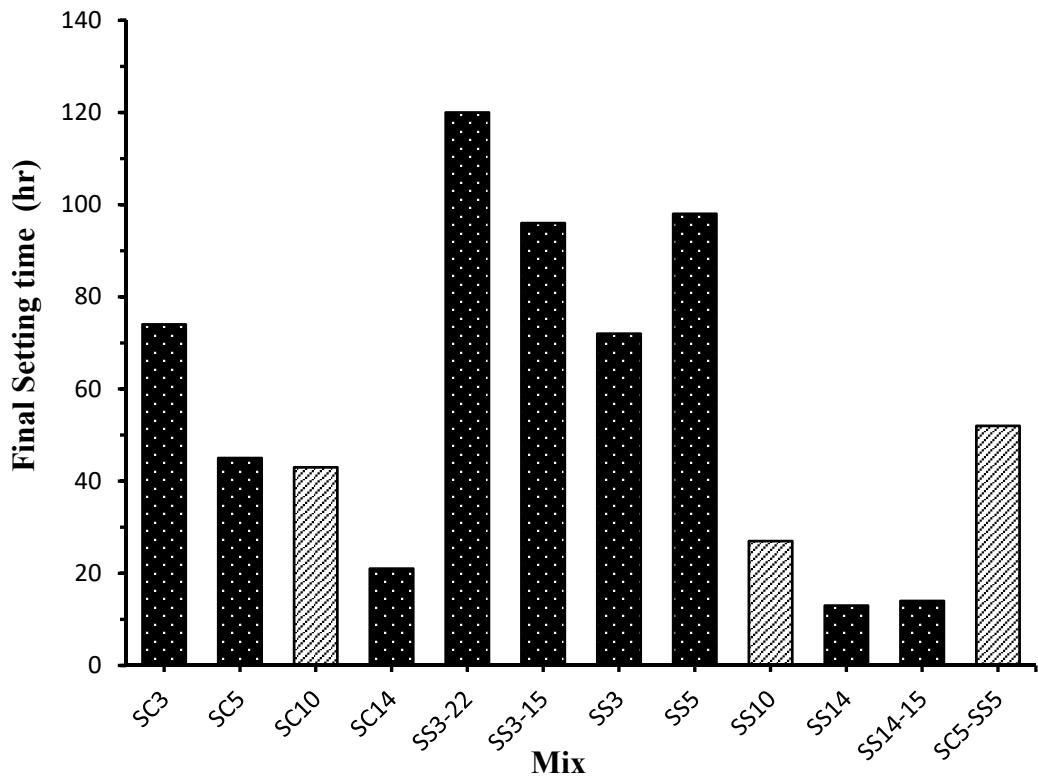
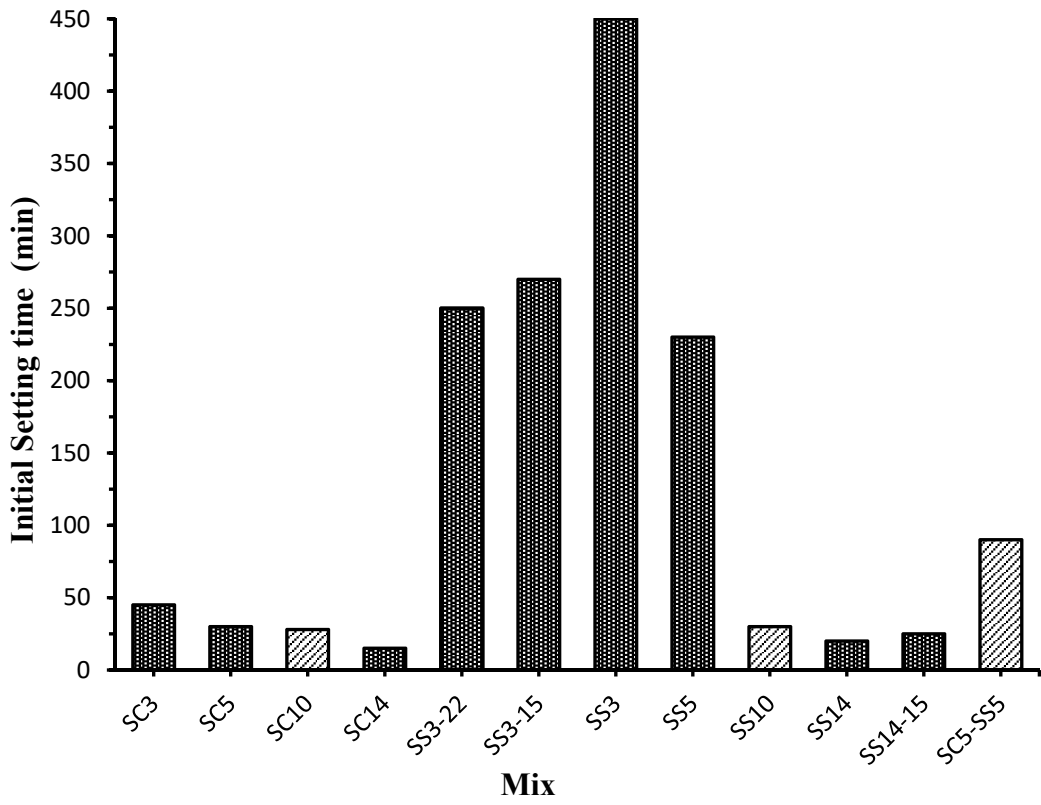


Figure 4: A: initial setting times for AAS pastes in minutes; B: final setting times for AAS pastes in hours.

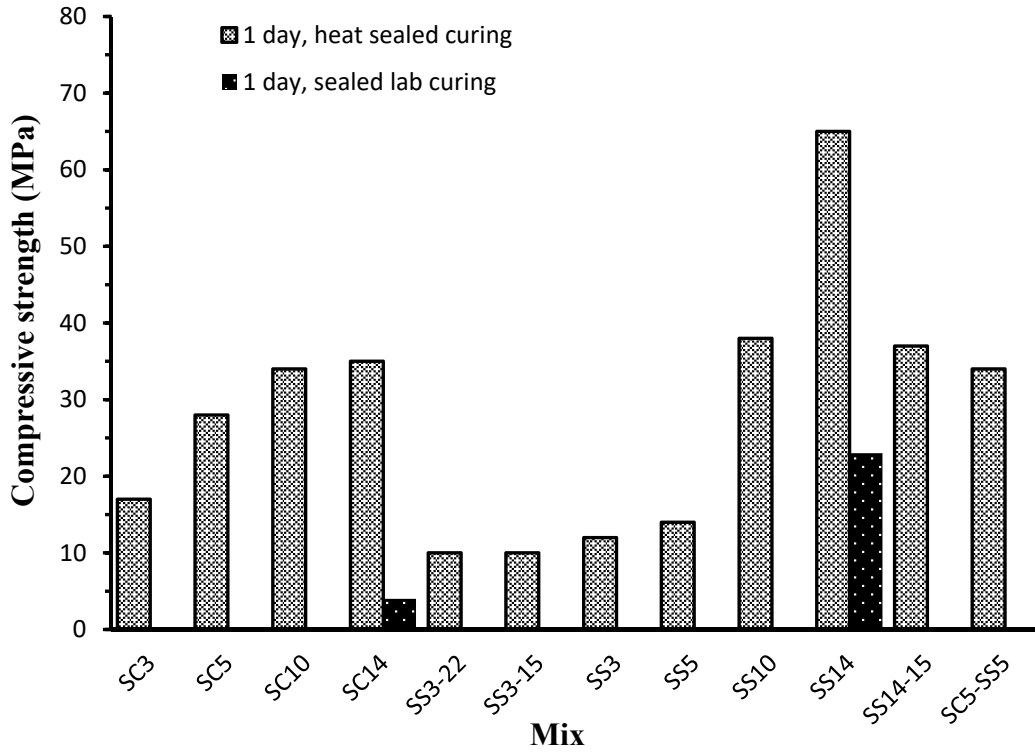


Figure 5: 1 day compressive cube strength results for concretes.

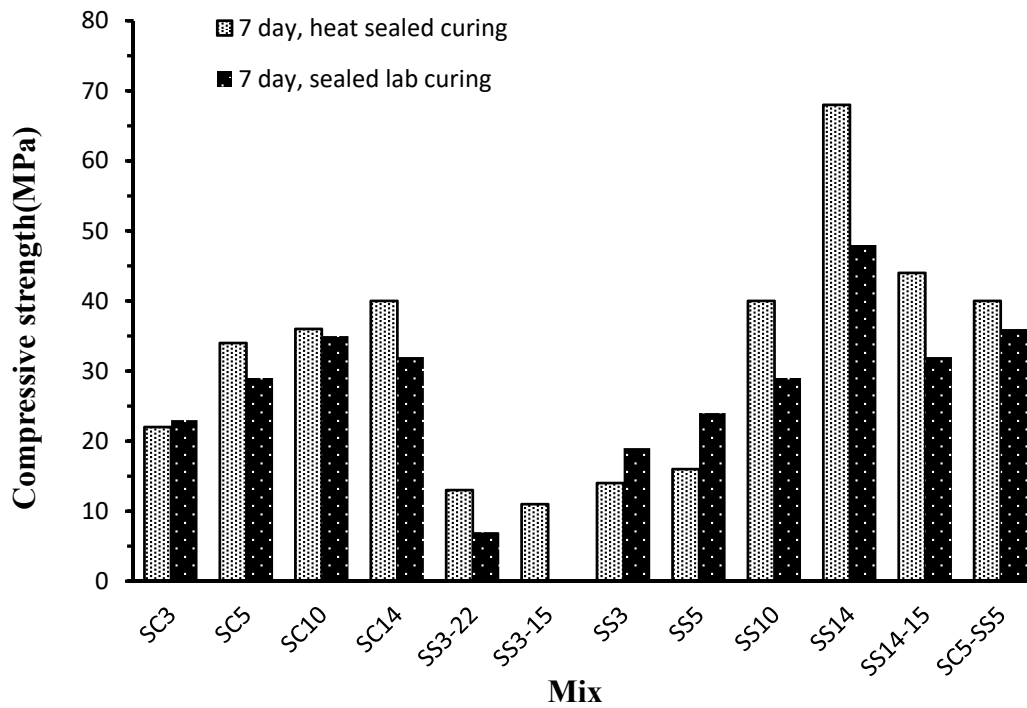


Figure 6: 7 day compressive cube strength results for concretes.

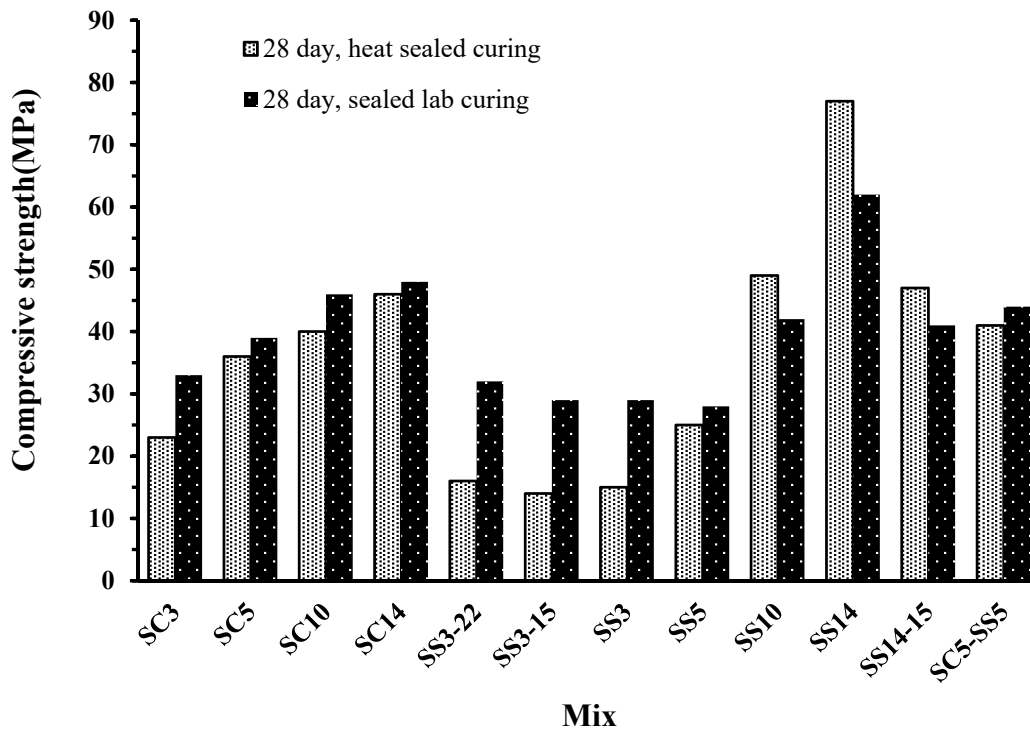


Figure 7: 28 day compressive strength results for concretes.

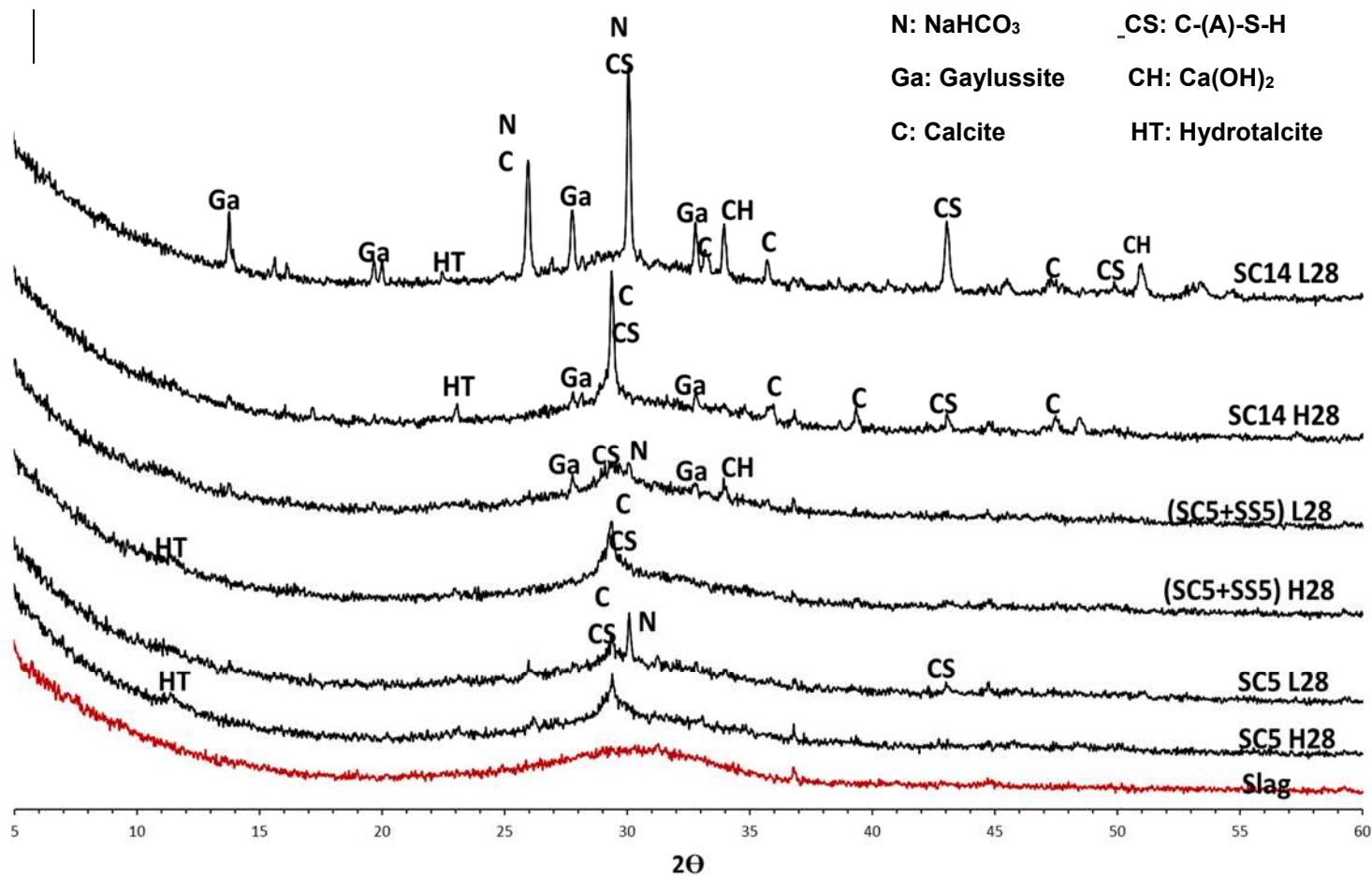


Figure 8: XRD results for 28 day old AAS pastes activated with SC. Suffix L28 denotes 28 days of lab curing and H28 denotes 28 days of heat curing.

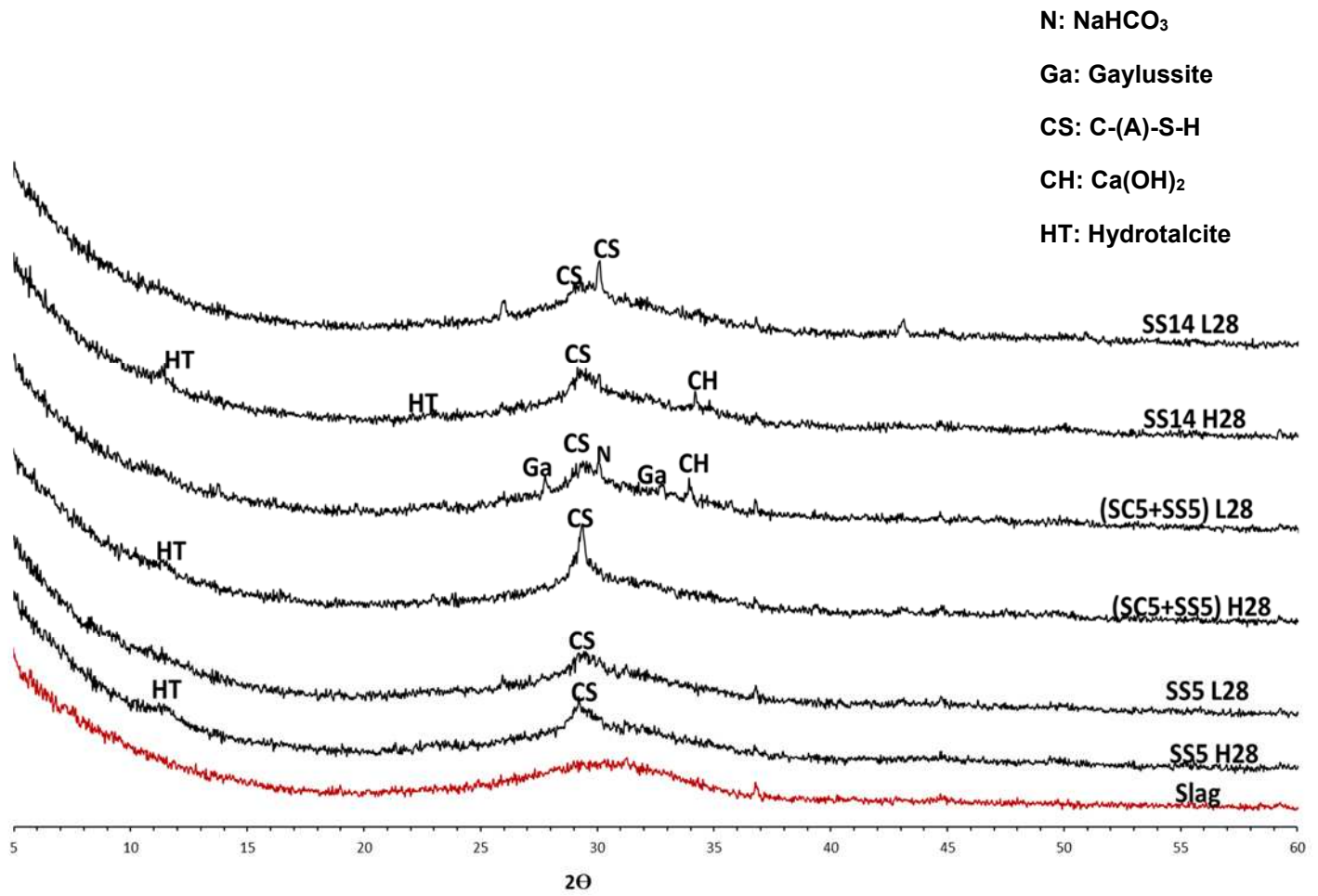


Figure 9: XRD results for 28 day old AAS pastes activated with SS. Suffix L28 denotes 28 days of lab curing and H28 denotes 28 days of heat curing.